

# Bovine Mitochondrial Peroxiredoxin III Forms a Two-Ring Catenane

Zhenbo Cao,<sup>1,2</sup> Aleksander W. Roszak,<sup>2</sup>  
Louise J. Gourlay,<sup>1</sup> J. Gordon Lindsay,<sup>1</sup>  
and Neil W. Isaacs<sup>2,\*</sup>

<sup>1</sup>Department of Biochemistry and Molecular Biology  
University of Glasgow  
Glasgow G12 8QQ  
United Kingdom

<sup>2</sup>WestCHEM  
Department of Chemistry  
University of Glasgow  
Glasgow G12 8QQ  
United Kingdom

## Summary

A crystal structure is reported for the C168S mutant of a typical 2-Cys peroxiredoxin III (Prx III) from bovine mitochondria at a resolution of 3.3 Å. Prx III is present as a two-ring catenane comprising two interlocking dodecameric toroids that are assembled from basic dimeric units. Each ring has an external diameter of 150 Å and encompasses a central cavity that is 70 Å in width. The concatenated dodecamers are inclined at an angle of 55°, which provides a large contact surface between the rings. Dimer-dimer contacts involved in toroid formation are hydrophobic in nature, whereas the 12 areas of contact between interlocked rings arise from polar interactions. These two major modes of subunit interaction provide important insights into possible mechanisms of catenane formation.

## Introduction

The peroxiredoxins (Prxs) are a ubiquitous family of antioxidant enzymes that regulate intracellular levels of H<sub>2</sub>O<sub>2</sub>, and they are implicated in both tissue protection against oxidative stress and H<sub>2</sub>O<sub>2</sub>-mediated signaling pathways (Wood et al., 2003). In recent years, their key role in antioxidant defense has been emphasized by their abundance in both bacterial and mammalian cells. Prxs can be classified as 1-Cys or 2-Cys Prxs based on the number of cysteine residues participating in catalysis (Chae et al., 1994). There is a further subdivision into two classes called the “typical” and “atypical” 2-Cys Prxs based on structural and mechanistic data. This diverse group of antioxidant enzymes is widespread in nature, with many organisms producing a number of isoforms. Thus, the group was further divided into six subclasses.

Typical 2-Cys Prxs function as thioredoxin-dependent hydroperoxide reductases and are organized as homodimers in which the adjacent subunits interact in a “head-to-tail” fashion. During the catalytic cycle, the N-terminal cysteine is oxidized to a cysteine sulphenic acid by its peroxide substrate, which subsequently forms an intersubunit disulphide bond with the con-

served C-terminal cysteine of its partner. Atypical 2-Cys Prxs exist as monomers or dimers and generate an intramolecular disulphide bond during the reaction (Seo et al., 2000). Crystal structures have now been reported for five atypical 2-Cys, eight typical 2-Cys, and four 1-Cys Prxs. In five of the typical 2-Cys structures, the basic dimeric unit is further assembled into decameric rings. In the remaining 2-Cys and 1-Cys Prxs, the structures are monomers or dimers, with two exceptions. Recently, an octameric organization has been reported for a 1-Cys Prx (Li et al., 2005), and another 2-Cys Prx from the same organism has been shown to exist as a dodecamer (Guimaraes et al., 2005). As the basic functional unit of all Prxs is either a monomer or a dimer, the precise relationship between peroxidase activity and the oligomeric state of these enzymes is unclear at present.

Peroxiredoxin III, or SP-22 (originally identified as a 22 kDa substrate protein for a mitochondrial ATP-dependent protease) (Watabe et al., 1994), is a typical member of the 2-Cys Prx III subclass with catalytic cysteines at its N(Cys47) and C(Cys168) termini. Electron microscopy (EM) studies (Gourlay et al., 2003; Wood et al., 2003) have shown that SP-22 exists as an oligomeric ring (previously thought to be decameric) enclosing a central cavity, although its overall dimensions are, in fact, slightly larger than those of other typical decameric Prx structures. We have now elucidated the crystal structure of the bovine mitochondrial SP-22 C168S mutant at 3.3 Å resolution, where it is found to be present as two interlocked dodecameric toroids.

## Results and Discussion

Wild-type SP-22 and its C168S mutant were overexpressed and purified as reported previously (Gourlay et al., 2003). Crystals of the mutant protein and a selenomethionine-substituted derivative of the mutant were grown from a high-concentration solution (38 mg/ml), with ammonium sulfate and isopropanol as precipitants. Diffraction data from the selenomethionine-substituted protein were collected to a resolution of 3.1 Å at three wavelengths around the Se absorption edge on BM14 at the ESRF. The crystals belong to the monoclinic space group C2 with the Matthews coefficient (Matthews, 1968), suggesting 10 ( $V_m = 2.8 \text{ \AA}^3/\text{Da}$ ) or 12 ( $V_m = 2.3 \text{ \AA}^3/\text{Da}$ ) monomeric subunits in the crystal asymmetric unit. The usual statistical indicators gave no indication of crystal twinning (see Figure S1 in the Supplemental Data available with this article online). A self-rotation function (see Figure S2) indicated the presence of two differently oriented dodecameric structures in the crystal. Initial attempts to solve the structure by molecular replacement were unsuccessful, as were efforts to locate the Se positions by using the Se-MAD data. A solution was finally obtained by the molecular replacement program PHASER (Storoni et al., 2004) by using the dimer of thioredoxin peroxidase B (PDB code 1qmv) as a search model. This solution was composed of two semicircular trimeric assemblies of the dimers. Upon applying the crystallographic 2-fold

\*Correspondence: n.isaacs@chem.gla.ac.uk

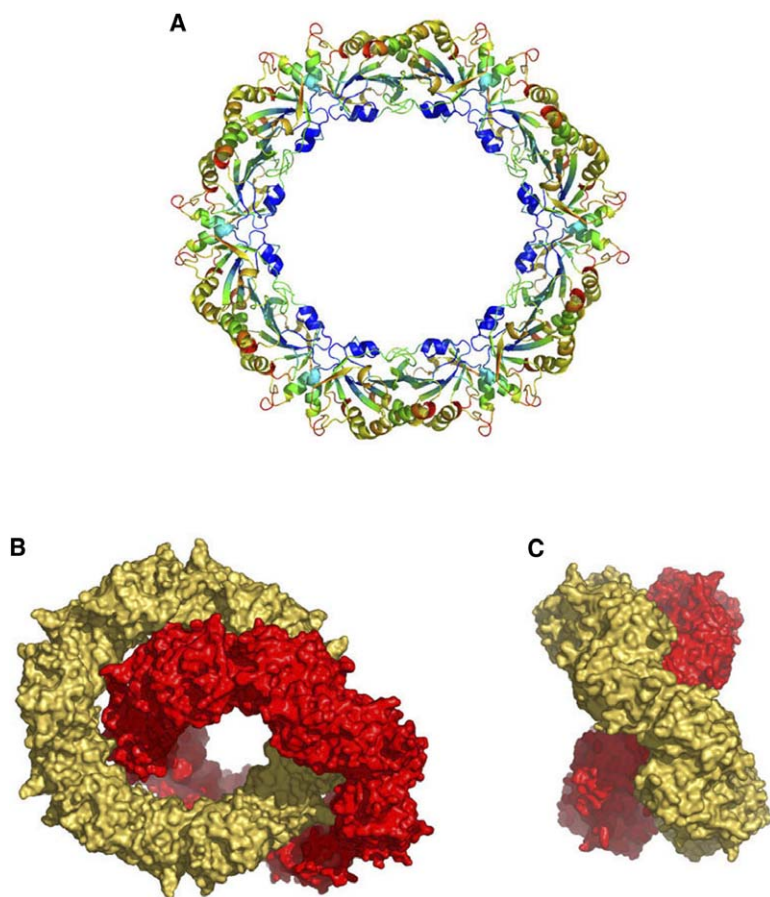


Figure 1. An Overview of the SP-22 C168S Structure

(A) The basic dodecameric SP-22 C168S toroid. Coloring is added by using atomic B factors.

(B) Surface diagram of the catenane structure of SP-22 C168S showing the two interlocking rings in red and gold, respectively.

(C) Side view of the two-ring catenane structure illustrating that the planes of the two rings lie at an angle of  $55^\circ$  to each other.

symmetry along the b axis, two interlocked dodecameric ring structures were formed. The structure, excluding the C-terminal 32 amino acids and the N-terminal residue, for which no model could be built in weak electron density, has been refined by using the program REFMAC5 (Murshudov et al., 1997) with tight NCS restraints. The  $R_{\text{work}}$  and  $R_{\text{free}}$  values are 0.223 and 0.265, respectively. No torsion angles fall into the disallowed region of the Ramachandran plot, and an analysis of the geometry and crystal packing with PROCHECK (Laskowski et al., 1993) shows no serious problems.

Monomeric SP-22 C168S is a compact globular structure, with the typical thioredoxin fold of the Prx family constructed around a seven-stranded, twisted  $\beta$  sheet surrounded by four  $\alpha$  helices. Stable dimers are formed across a noncrystallographic 2-fold axis that extends the central  $\beta$  sheet and buries a total of  $1772 \text{ \AA}^2$  of solvent-accessible surface ( $886 \text{ \AA}^2$  per monomer). This monomer-monomer interface is similar to that formed in other typical 2-Cys Prx structures and corresponds to the B-type interface (Sarma et al., 2005).

The 6-fold NCS-related dimers are assembled into a dodecameric ring structure with outer and inner diameters of 150 and 70  $\text{\AA}$ , respectively (cf. 130 and 60  $\text{\AA}$  for the decameric Prxs) (Figure 1A). The dimer-dimer interfaces within the ring are formed mainly by hydrophobic residues (Leu41, Phe43, Phe45, Val73, Phe77, Leu103, Leu120) burying  $635 \text{ \AA}^2$  of solvent-accessible surface per monomer, also similar to the A-type interface (Sarma et al., 2005). A similar dodecameric ring structure has

recently been reported for the crystal structure of MtAhpC<sub>176S</sub> (Guimaraes et al., 2005). This, and our results, shows that 2-Cys Prx oligomers are not restricted to forming decameric toroids.

The most surprising feature of the crystal structure of SP-22 C168S is its presence as a two-ring catenane comprising two interlocking dodecameric toroids (Figure 1B). The planes of the rings are not at right angles, but are inclined at an angle of  $55^\circ$  (Figure 1C), which allows a larger contact surface between the rings. This arrangement explains a large peak in the self-rotation function at  $\chi = 55^\circ$  with a coincident 2-fold NCS axis (see Figure S2). There are 12 areas of contact, burying  $5067 \text{ \AA}^2$  of solvent-accessible surface, between the rings. These contacts arise from four NCS-related copies of three distinct interfaces. The prominent feature of the first contact area is Lys88, which projects into a polar cavity at the dimer-dimer interface and forms a hydrogen bond with Thr104 (Figure 2B). The second contact area is stabilized by a pair of 2-fold NCS-related hydrogen bonds between Lys12 and Tyr10 (Figure 2D). The contacts in the third area are also polar (Figure 2C). A salt bridge is formed between Arg109 and Glu67, but other hydrogen bond contacts cannot be defined due to the resolution and accuracy of the structure.

To date, there have been only two reports describing the presence of true topological links between protein molecules. In the 420-meric bacteriophage HK97 capsid, each subunit is bound to two of its neighbors by an isopeptide bond between Lys169 and Asn356. This

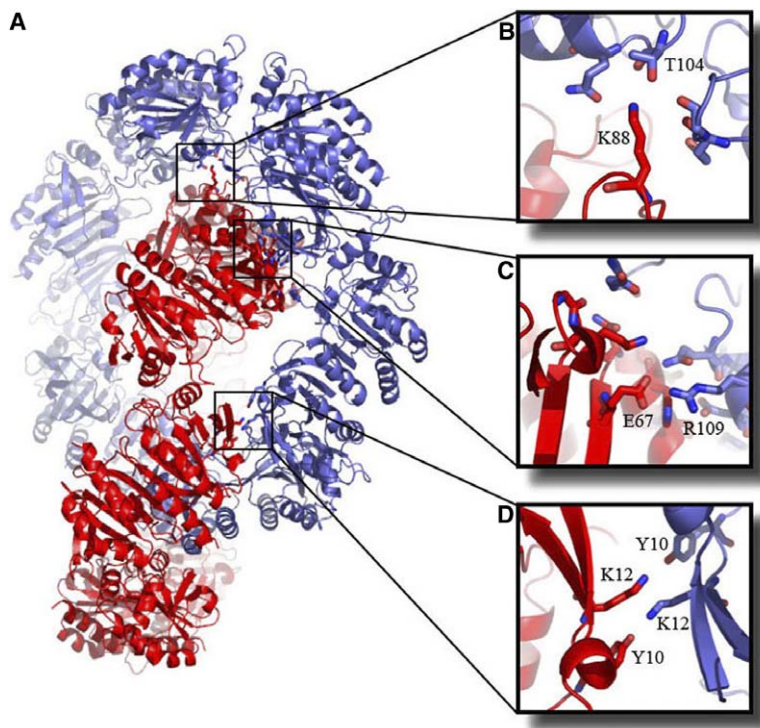


Figure 2. Sites of Interaction between the Two Interlocked Rings

(A) An overview of the three main sites of polar contact between the two interlocked dodecameric rings depicted in red and blue, respectively. These are each replicated four times in the overall structure.

(B–D) Detailed representation of the polar contacts between the two rings. (B) The hydrogen bond between K88 and Thr104 located in a polar cavity. (C) Salt bridge between E67 and R109. (D) 2-fold related hydrogen bonds between K12 and Y10.

conformation generates rings of covalently joined subunits, creating a form of protein “chain mail” (Wikoff et al., 2000). In another case, peptide synthesis and chemical ligation has been employed to produce a small, artificial protein catenane encoding a segment of a dimeric mutant of the p53tet protein (Yan and Dawson, 2001). However, to our knowledge, SP-22 C168S represents the first observed example of a classical, naturally occurring, interlocked two-ring protein structure, a protein catenane.

Preliminary data from analytical ultracentrifugation (AUC) and EM studies indicate that the SP-22 C168S preparations employed for crystallization contain a mixed population of single- and double-ring oligomers (data not shown). We have no data indicating how the two-ring catenane structure is formed, but the crystal structure does provide some important insights into possible mechanisms of assembly. Dimeric units can interact in two different modes that are not mutually exclusive. One mode produces the dimer-dimer contacts, primarily hydrophobic, associated with ring generation in this and other Prx structures (Sarma et al., 2005). The other mode gives polar contacts that could potentially initiate catenane formation at any stage during single toroid assembly by allowing two rings to form simultaneously around each other. A general model illustrating

catenane formation arising from polar contacts between two basic dimeric units is shown in Figure 3. At present, it is unclear whether the fraction of the mixed population represented by the concatenated rings is assembled in vivo during overexpression in *E. coli*, or whether it arises as a result of increasing protein concentration. A likely scenario is that interlocked double rings, single rings, and a small population of dimers are in dynamic equilibrium in solution, so that during the crystallization process in vitro, where there is a very high concentration of protein, formation of crystals from the catenated rings would be the most favored event.

At present, we are unsure if this assembly has any physiological relevance. However, the novel architecture of this naturally occurring, two-ring catenane may provide interesting new insights into protein topology and mechanisms of subunit assembly.

#### Experimental Procedures

##### Protein Purification and Crystallization

Purified protein, subjected to gel filtration chromatography as described previously (Gourlay et al., 2003) in 50 mM NaCl, 20 mM HEPES (pH 7.2), 10 mM dithiothreitol (DTT), and 5 mM EDTA, was used directly for crystallization. Crystallization trials were performed at 16°C by using the sitting-drop vapor-diffusion method. Wild-type SP-22 gave only microcrystals, unsuitable for X-ray diffraction

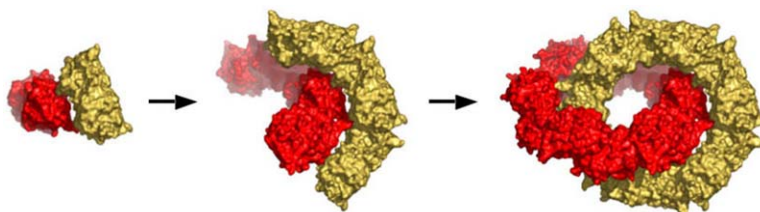


Figure 3. General Model for Mechanism of Assembly of the Two-Ring Catenane Structure  
Polar contacts between adjacent dimers (shown in red and gold), potentially occurring at any stage during single toroid formation, provide the basis for initiating the generation of a second topologically linked ring, leading to the overall two-ring catenane structure.

Table 1. Data Collection and Refinement Statistics

Data Collection	
Space group	C2
Unit cell dimensions (Å)	a = 301.0; b = 80.7; c = 124.3
$\beta$ (°)	112.8
Resolution (Å) <sup>a</sup>	35.8–3.3 (3.5–3.3)
Total/unique observations	314,446/41,825
Completeness (%) <sup>a</sup>	99.9 (100)
Multiplicity <sup>a</sup>	7.5 (7.6)
R <sub>merge</sub> (%) <sup>a</sup>	12.2 (50.7)
Mean I/σ(I) <sup>a</sup>	5.1 (1.3)
Refinement	
R <sub>work</sub> /R <sub>free</sub> (%)	22.3/26.5
Rms deviations	
Bond lengths (Å)	0.019
Bond angles (°)	1.76
Ramachandran plot (%)	
Core region	89.0
Allowed	9.3
Generously allowed	1.7
Forbidden	0

<sup>a</sup>Values in parentheses refer to the final resolution shell.

studies. The best crystals of SP-22 C168S, obtained from drops composed of 2 μl protein solution (38 mg/ml) mixed with a 2 μl volume of a 1 ml reservoir solution containing 1.65 M ammonium sulfate and 5% isopropanol, grew to a size of 0.5 × 0.2 × 0.2 mm in a week.

#### Data Collection

The mother liquor with 25% (v/v) glycerol was used as a cryoprotectant. X-ray diffraction data sets were collected at 100 K by using synchrotron radiation (European Synchrotron Radiation Facility, Grenoble, France) at the BM14 beamline equipped with a MARMOSAIC225 CCD detector. The wavelength was set at 0.979 Å for the peak of the Se anomalous dispersion signal. A total of 720 frames were recorded with a crystal detector distance of 325 mm and 0.5° of oscillation. All data were processed to a resolution of 3.3 Å by using the programs MOSFLM, SCALA, and TRUNCATE from the CCP4 package (CCP4, 1994). Data collection statistics are summarized in Table 1. The acentric moments statistics produced by SCALA (see Figure S1) show no indications of crystal twinning.

#### Structure Determination

A self-rotation function, calculated by the program MOLREP with data in the 10–4 Å resolution range and an integration radius of 30 Å, showed two clear 6-fold symmetry axes, each perpendicular to six 2-fold symmetry axes, indicating two conformations of dodecamer structures in the crystal (see Figure S2). An initial phase set was obtained by molecular replacement with the program PHASER (Storoni et al., 2004) by using a dimer of thioredoxin peroxidase B (PDB code 1qmv) as a search model to locate three dimers. This gave a solution locating a semicircular, trimeric assembly of dimers. Upon searching for another hexamer, a second independent half ring was found. Applying the crystallographic 2-fold symmetry along the b axis to these solutions gives two interlocked dodecameric ring structures. This structure was refined in ten cycles of rigid-body refinement, with a dodecameric ring treated as 12 domains, by using the program REFMAC5 (Murshudov et al., 1997). Several more rounds of restrained refinement with tight NCS restraints reduced R<sub>work</sub> to 0.223 and R<sub>free</sub> to 0.265 with good stereochemistry (Table 1). All figures were drawn by PyMOL (Delano, 2002).

#### Supplemental Data

Supplemental Data including Figures S1 and S2 are available at <http://www.structure.org/cgi/content/full/13/11/1661/DC1/>.

#### Acknowledgments

We thank Hassan Belrhali and Karen McLuskey for assistance with data collection at station BM14, European Synchrotron Radiation

Facility, France. This work was supported by the Biotechnology and Biological Sciences Research Council and the Wellcome Trust. Z.C. gratefully acknowledges the award of a Wellcome Trust post-graduate studentship.

Received: July 1, 2005

Revised: July 29, 2005

Accepted: July 29, 2005

Published: November 8, 2005

#### References

- CCP4 (Collaborative Computational Project, Number 4) (1994). The CCP4 suite: programs for protein crystallography. *Acta Crystallogr. D Biol. Crystallogr.* **50**, 760–763.
- Chae, H.Z., Robison, K., Poole, L.B., Church, G., Storz, G., and Rhee, S.G. (1994). Cloning and sequencing of thiol-specific antioxidant from mammalian brain: alkyl hydroperoxide reductase and thiol-specific antioxidant define a large family of antioxidant enzymes. *Proc. Natl. Acad. Sci. USA* **91**, 7017–7021.
- Delano, W.L. (2002). The PyMOL Molecular Graphics System (San Carlos, CA: Delano Scientific).
- Gourlay, L.J., Bhella, D., Kelly, S.M., Price, N.C., and Lindsay, J.G. (2003). Structure-function analysis of recombinant substrate protein 22 kDa (SP-22). A mitochondrial 2-Cys peroxiredoxin organized as a decameric toroid. *J. Biol. Chem.* **278**, 32631–32637.
- Guimaraes, B.G., Souchon, H., Honore, N., Saint-Joanis, B., Brosch, R., Shepard, W., Cole, S.T., and Alzari, P.M. (2005). Structure and mechanism of the alkyl hydroperoxidase AhpC, a key element of the *Mycobacterium tuberculosis* defense system against oxidative stress. *J. Biol. Chem.* **280**, 25735–25742.
- Laskowski, R.A., MacArthur, M.W., Moss, D.S., and Thornton, J.M. (1993). Procheck - a program to check the stereochemical quality of protein structures. *J. Appl. Crystallogr.* **26**, 283–291.
- Li, S., Peterson, N.A., Kim, M.Y., Kim, C.Y., Hung, L.W., Yu, M., Lakin, T., Segelke, B.W., Lott, J.S., and Baker, E.N. (2005). Crystal structure of AhpE from *Mycobacterium tuberculosis*, a 1-Cys peroxiredoxin. *J. Mol. Biol.* **346**, 1035–1046.
- Matthews, B.W. (1968). Solvent content of protein crystals. *J. Mol. Biol.* **33**, 491–497.
- Murshudov, G.N., Vagin, A.A., and Dodson, E.J. (1997). Refinement of macromolecular structures by the maximum-likelihood method. *Acta Crystallogr. D Biol. Crystallogr.* **53**, 240–255.
- Sarma, G.N., Nickel, C., Rahlfs, S., Fischer, M., Becker, K., and Karplus, P.A. (2005). Crystal structure of a novel *Plasmodium falciparum* 1-Cys peroxiredoxin. *J. Mol. Biol.* **346**, 1021–1034.
- Seo, M.S., Kang, S.W., Kim, K., Baines, I.C., Lee, T.H., and Rhee, S.G. (2000). Identification of a new type of mammalian peroxiredoxin that forms an intramolecular disulfide as a reaction intermediate. *J. Biol. Chem.* **275**, 20346–20354.
- Storoni, L.C., McCoy, A.J., and Read, R.J. (2004). Likelihood-enhanced fast rotation functions. *Acta Crystallogr. D Biol. Crystallogr.* **60**, 432–438.
- Watabe, S., Kohno, H., Kouyama, H., Hiroi, T., Yago, N., and Nakazawa, T. (1994). Purification and characterization of a substrate protein for mitochondrial ATP-dependent protease in bovine adrenal cortex. *J. Biochem. (Tokyo)* **115**, 648–654.
- Wikoff, W.R., Liljas, L., Duda, R.L., Tsuruta, H., Hendrix, R.W., and Johnson, J.E. (2000). Topologically linked protein rings in the bacteriophage HK97 capsid. *Science* **289**, 2129–2133.
- Wood, Z.A., Schroder, E., Robin Harris, J., and Poole, L.B. (2003). Structure, mechanism and regulation of peroxiredoxins. *Trends Biochem. Sci.* **28**, 32–40.
- Yan, L.Z., and Dawson, P.E. (2001). Design and synthesis of a protein catenane. *Angew. Chem. Int. Ed. Engl.* **40**, 3625–3627.

#### Accession Numbers

The atomic coordinates and structure factors have been deposited with the Protein Data Bank with accession number 1ZYE.